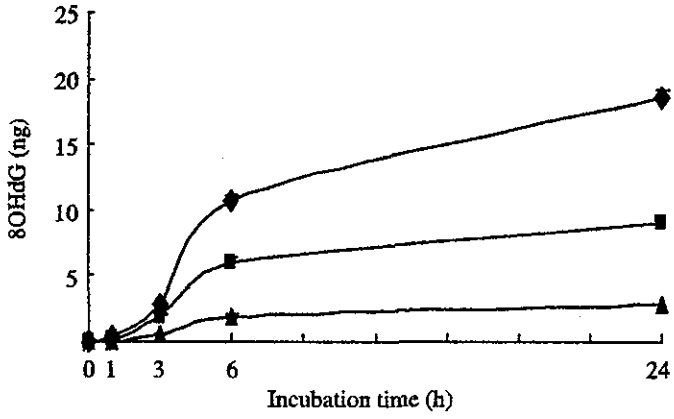

Fig. 2. Time course of 8-hydroxydeoxyguanosine (8OHdG) generation from DNA with different levels of 8OHdG. Ultraviolet irradiation with (◆) 50 μg/mL, (■) 10 μg/mL or (▲) 2 μg/mL riboflavin-damaged DNA samples were incubated with rat liver homogenates at 37°C for 1, 3, 6, or 24 h. Then the incubation mixtures were ultrafiltered through YM10 and the quantities of 8OHdG in the ultrafiltrates were determined as described in Materials and Methods. Results from a typical experiment conducted in triplicate is presented as mean ± SE.

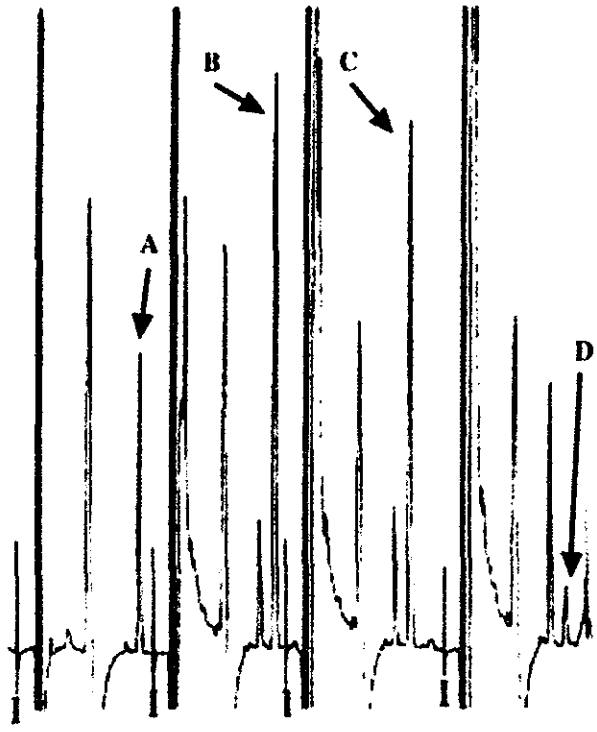

Fig. 3. High-performance liquid chromatography–electrochemical detector chromatogram of the final ultrafiltrates incubated with anti-8-hydroxydeoxyguanosine (8OHdG) antibody or control IgG1. After incubation of DNA (damaged by ultraviolet irradiation with 50 μg/mL riboflavin) with rat liver homogenates at 37°C for 18 h, the incubation mixture was ultrafiltered. The ultrafiltrate was incubated with Dulbecco's phosphate-buffered saline (B), control IgG1 (C), or anti-8OHdG antibody (D), then the mixtures were ultrafiltered again with YM10. Quantities of 8OHdG in the final ultrafiltrates were determined as described in Materials and Methods. Peak A indicates authentic 8OHdG, and 'I' indicates the injection points of samples.

time as authentic 8OHdG. Control IgG1 did not absorb the peak in the ultrafiltrate; however, anti-8OHdG antibody at the same concentration as control IgG1 absorbed the peak almost completely.

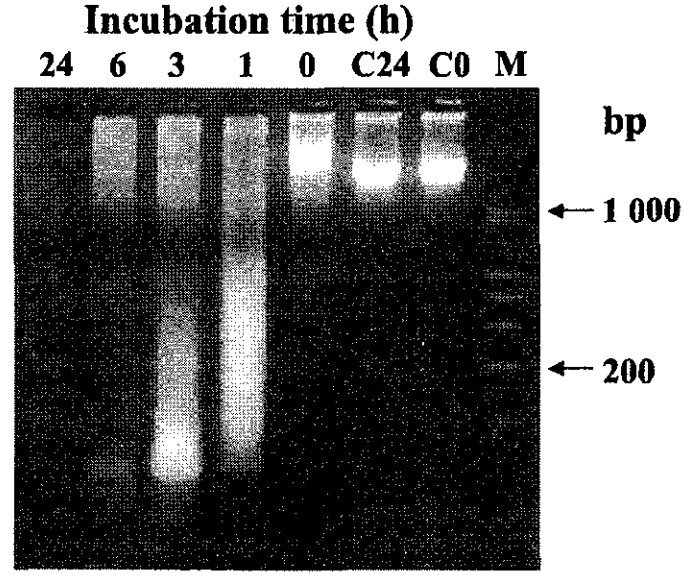

Fig. 4. Electrophoretic determination of DNA degradation by rat liver homogenates. DNA (damaged by ultraviolet irradiation with 50 μg/mL riboflavin) was incubated with rat liver homogenates at 37°C for the indicated durations. Then incubation mixtures containing 1.0 μg DNA were subjected to electrophoresis as described in Materials and Methods. C0, C24: samples of damaged DNA were incubated with homogenization buffer at 37°C for 0 h (C0) or 24 h (C24). M, marker DNA fragments, sizes of marker fragments are indicated on the right.

Degradation of DNA by rat liver homogenates. As Figure 4 shows, rat liver homogenates degraded DNA that had been damaged by UV irradiation in the presence of 50 μg/mL riboflavin. Oxidatively damaged DNA was considerably degraded even after 1 h of incubation, and the DNA degradation by rat liver homogenates was dependent on the incubation time. In contrast, when damaged DNA was incubated for 24 h without rat liver homogenates, it was not degraded (C24 *vs* C0). Although the DNA was extensively damaged by UV irradiation in the presence of riboflavin, its size was larger than 1000 bp (C0).

Changes in the amount of dG, 8OHG or 8OHdG in the presence of rat liver homogenates. As Figure 5A shows, when dG was incubated with rat liver homogenates, a small amount of 8OHdG was detected at 0 h of incubation, and this amount increased slightly after 6 h of incubation. At 6 h, however, the amount of 8OHdG generated from dG was <1/10 000 of dG (Fig. 5A). In the presence of rat liver homogenates, dG disappeared rapidly. More than 70% of dG had disappeared even after 0.5 h of incubation: after 3 h none could be detected. By contrast, in the presence of rat liver homogenates, 8OHG and 8OHdG did not breakdown significantly after 6 h, and more than 75% of 8OHG and 8OHdG were detected unchanged even after 24 h of incubation (Fig. 5B,C). 8OHdG was not generated from 8OHG by rat liver homogenates.

Discussion

Urinary 8OHdG is widely used as a biological marker with which to evaluate oxidative stress in the body.[22,34,35] Its usefulness, however, has so far been limited because we do not know enough about how 8OHdG comes to be present in urine.[23,31] No evidence has been presented that 8OHdG is released from DNA by tissues, cells, or by their extracts. Here, the authors clearly show that 8OHdG is generated from DNA by rat liver homogenates (Fig. 1). Because other compounds that are present in rat liver homogenates might have, in HPLC analysis, produced peaks at the same position as 8OHdG, the authors tested with an anti-8OHdG antibody. The antibody absorbed the peak almost

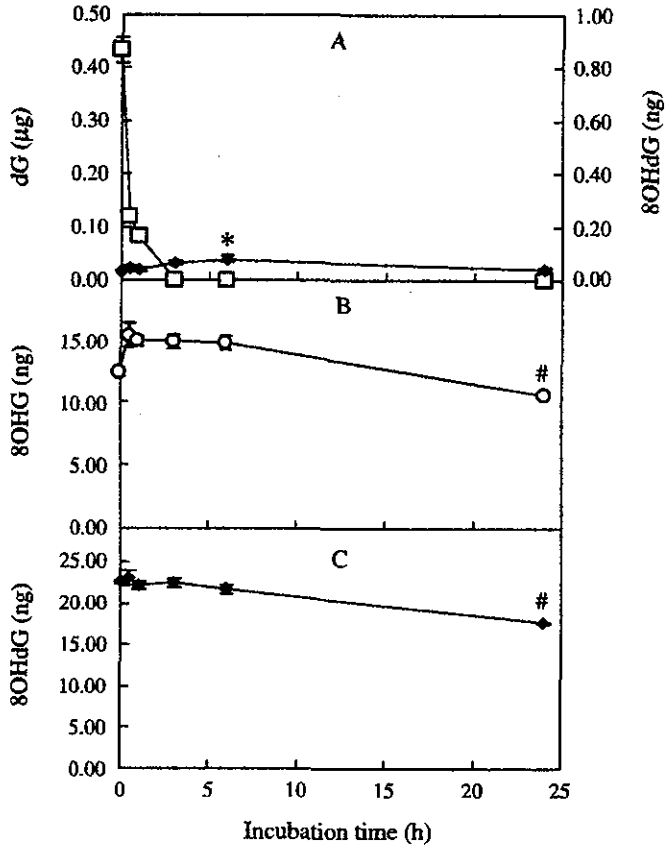

Fig. 5. Effect of incubation time on (□) quantity of deoxyguanosine (dG), (○) 8-hydroxyguanine (8OHG), or (◆) 8-hydroxydeoxyguanosine (8OHdG) in the presence of rat liver homogenates. (A) dG (0.5 μg). (B) 8OHG (16 ng). (C) 8OHdG (25 ng). Amounts were calculated from samples of 10 μg of DNA that were damaged by ultraviolet irradiation with 50 μg/mL riboflavin. These were incubated at 37°C with rat liver homogenates for 0, 0.5, 1, 3, 6 or 24 h. After incubation, the mixtures were ultrafiltered and the quantities of dG, 8OHG, or 8OHdG in the ultrafiltrates were determined as described in Materials and Methods. Data from a typical experiment conducted in triplicate are presented as mean ± SE. *$P < 0.05$, significantly increased when compared with 0 h; #$P < 0.05$, significantly decreased when compared with 0 h.

completely, indicating that 8OHdG was generated from DNA (Fig. 3). Our data also show that the quantity of 8OHdG generated from the DNA corresponds with the level of oxidative damage in the DNA (Fig. 2). These findings indicate that, *in vivo*, 8OHdG is generated from DNA, and that the amounts of generated 8OHdG are useful for evaluating oxidative damage in DNA. However, attention should be paid when determining the 8OHdG quantity (see Fig. 2).

A semiquantitative assay of 8OHG using the 8OHdG detection system showed that the quantities of 8OHG produced from DNA were approximately 1/25 of the quantities of 8OHdG after incubation of DNA with rat liver homogenates, and that the proportion did not vary with the 8OHdG levels in DNA (data not shown). It might be thought that just 70% of 8OHdG was released from DNA after a 24-h incubation period (Table 1). However, Figure 5C shows that 75% of 8OHdG could be recovered after the same incubation time in the presence of rat liver homogenates. Thus, in this system, the authors considered that most of the 8OHdG in damaged DNA was released as 8OHdG.

The authors were surprised that most of the 8OHdG was released from DNA by the rat liver homogenates. At first, it was considered that 8OHdG was generated during the DNA repair process, because dG, a DNA degradation product,[1] was barely detectable in the ultrafiltrates. The result of electrophoresis (Fig. 4), however, indicated that the generation of 8OHdG co-occurred during DNA degradation. In the presence of rat liver homogenates, it is possible that dG rapidly disappeared, which was confirmed as shown in Figure 5A. When DNA was incubated with rat liver homogenates for 1 h, the electrophoretic mobility of oxidatively damaged DNA was decreased, probably due to the interaction between the DNA and the proteins in the homogenate.

It is also possible that 8OHdG is generated from dG or 8OHG. In particular, generation from dG has been reported in the co-presence of oxidants.[9,36,37] Commercially available dG preparations usually contain 1–5 molecules of 8OHdG per 100 000 of dG (data not shown). When dG was incubated with rat liver homogenates, however, <1/10 000 of the dG was converted to 8OHdG during 6 h of incubation (Fig. 5A). Meanwhile, 8OHdG was not generated when 8OHG was incubated with rat liver homogenates (Fig. 5B). These findings indicate that, during DNA degradation, 8OHdG was generated directly from DNA. The authors suggest that 8OHdG is generated when oxidative stress causes tissue or cell destruction: in such conditions, both oxidative DNA damage and tissue or cell homogenates could be produced. Because oxidative stress induces apoptosis,[38,39] and DNA is extensively degraded during apoptosis,[40] apoptotic cells might also be sources of 8OHdG. The authors are now investigating whether living cells could also generate 8OHdG from DNA using a cell culture system.

Liver contains many types of nuclease[41–44] that degrade DNA to nucleotides. In turn, these can be dephosphorylated to nucleosides by the phosphatases that are also present in the liver.[45,46] Some nucleases in the liver are reported to be sensitive to NaCl,[47,48] and when NaCl was added to the incubation mixtures, NaCl at concentrations of more than 150 mmol/L inhibited the generation of 8OHdG (data not shown). The finding further supports our conclusion that 8OHdG generation is coupled with DNA degradation. Thus it seems plausible that, in the present experiment, the nucleases and phosphatases present in the liver were responsible for the generation of 8OHdG from DNA. Additionally, in support of this conclusion, the technique for determining 8OHdG in DNA uses nuclease P1, an exonuclease, and alkaline phosphatase.[11,33,49] Further study, however, is required to identify which enzyme or enzymes are responsible for the generation of 8OHdG from DNA. Furthermore, investigation as to which organ most efficiently generates 8OHdG may eventually make it possible to use urinary 8OHdG to evaluate organ-specific oxidative stress. In contrast to rat liver homogenates, Fpg protein, a bacterial homolog of oxoguanine glycosylase that acts as a DNA BER enzyme,[50,51] generated 8OHG from DNA, but not 8OHdG (data not shown).

It is interesting that, while dG rapidly disappeared under the same conditions, in the presence of rat liver homogenates more than 75% of 8OHG and 8OHdG remained unchanged up to 24 h of incubation (Fig. 5). These findings suggest that 8OHdG and 8OHG are stable in the body and in the circulation, and so may be excreted into urine unchanged, whereas most of dG undergoes breakdown and may not be detectable in urine as intact dG. This hypothesis is supported by the finding that the quantities of 8OHdG and 8OHG in urine are greatly disproportionate to the quantity of dG in urine.[18,22,52] It is also interesting that 8OHdG and 8OHG seem not to be metabolized or reused, suggesting the presence of mechanisms that do not allow the naturally occurring damaged base to be incorporated into nucleic acids. Our discovery of the stability of 8OHdG in the presence of rat liver homogenates suggests a useful substrate that could be used to study nucleases. Because 8OHdG is a stable product of nuclease reaction and can be determined with high sensitivity, DNA with 8OHdG seems to be a better substrate than DNA without 8OHdG.

 doi: 10.1111/j.1349-7006.2005.00004.x

In conclusion, 8OHdG is released from DNA by rat liver homogenates in quantities that correspond with the levels of oxidative damage in the DNA. Because 8OHdG is stable in the presence of rat liver homogenates, it is likely that 8OHdG is stable enough in circulation to be excreted into urine. Thus, urinary 8OHdG, if determined at appropriate times or with 24-h urine testing, is a useful marker of oxidative DNA damage that is induced by oxidative stress, particularly oxidative stress that leads to the organ or cell destruction, or apoptosis. Although the present results do not show the *in vivo* generation of 8OHdG from DNA directly, they show that 8OHdG is generated from DNA by a biological material, rat liver homogenate.

Acknowledgments

This work was supported by Grand-in-Aid for Scientific Research awarded by the Ministry of Education, Science, Sports and Culture of Japan (#14370140).

The authors express thanks to Professor Kanehisa Morimoto (Department of Social and Environmental Medicine, Course of Social Medicine, Osaka University Graduate School of Medicine) for his encouragement and support of this work.

References

1 Lindahl T. Instability and decay of the primary structure of DNA. *Nature* 1993; **362**: 709–15.
2 Beckman KB, Ames BN. Oxidative decay of DNA. *J Biol Chem* 1997; **272**: 19633–6.
3 Halliwell B, Gutteridge JMC. *Free Radicals in Biology and Medicine*. Oxford: Oxford University Press, 1999.
4 Halliwell B, Aruoma OI. DNA damage by oxygen-derived species. Its mechanism and measurement in mammalian systems. *FEBS Lett* 1991; **281**: 9–19.
5 Ames BN. Dietary carcinogens and anticarcinogens. Oxygen radicals and degenerative diseases. *Science* 1983; **221**: 1256–64.
6 Zhang J, Perry G, Smith MA, Robertson D, Olson SJ, Graham DG, Montine TJ. Parkinson's disease is associated with oxidative damage to cytoplasmic DNA and RNA in substantia nigra neurons. *Am J Pathol* 1999; **154**: 1423–9.
7 Shibutani S, Takeshita M, Grollman AP. Insertion of specific bases during DNA synthesis past the oxidation-damaged base 8-oxodG. *Nature* 1991; **349**: 431–4.
8 Cheng KC, Cahill DS, Kasai H, Nishimura S, Loeb LA. 8-Hydroxyguanine, an abundant form of oxidative DNA damage, causes G—T and A—C substitutions. *J Biol Chem* 1992; **267**: 166–72.
9 Floyd RA, Watson JJ, Wong PK, Altmiller DH, Rickard RC. Hydroxyl free radical adduct of deoxyguanosine: sensitive detection and mechanisms of formation. *Free Radic Res Commun* 1986; **1**: 163–72.
10 Kasai H. Analysis of a form of oxidative DNA damage, 8-hydroxy-2′-deoxyguanosine, as a marker of cellular oxidative stress during carcinogenesis. *Mutat Res* 1997; **387**: 147–63.
11 Foksinski M, Kotzbach R, Szymanski W, Olinski R. The level of typical biomarker of oxidative stress 8-hydroxy-2′-deoxyguanosine is higher in uterine myomas than in control tissues and correlates with the size of the tumor. *Free Radic Biol Med* 2000; **29**: 597–601.
12 Floyd RA. The role of 8-hydroxyguanine in carcinogenesis. *Carcinogenesis* 1990; **11**: 1447–50.
13 Kasai H, Crain PF, Kuchino Y, Nishimura S, Ootsuyama A, Tanooka H. Formation of 8-hydroxyguanine moiety in cellular DNA by agents producing oxygen radicals and evidence for its repair. *Carcinogenesis* 1986; **7**: 1849–51.
14 Collins AR, Gedik CM, Olmedilla B, Southon S, Bellizzi M. Oxidative DNA damage measured in human lymphocytes: large differences between sexes and between countries, and correlations with heart disease mortality rates. *FASEB J* 1998; **12**: 1397–400.
15 Yoshida R, Ogawa Y, Kasai H. Urinary 8-oxo-7,8-dihydro-2′-deoxyguanosine values measured by an ELISA correlated well with measurements by high-performance liquid chromatography with electrochemical detection. *Cancer Epidemiol Biomarkers Prev* 2002; **11**: 1076–81.
16 Tagesson C, Kallberg M, Klintenberg C, Starkhammar H. Determination of urinary 8-hydroxydeoxyguanosine by automated coupled-column high performance liquid chromatography: a powerful technique for assaying in vivo oxidative DNA damage in cancer patients. *Eur J Cancer* 1995; **31**: 934–40.
17 Lin HS, Jenner AM, Ong CN, Huang SH, Whiteman M, Halliwell B. A high-throughput and sensitive methodology for the quantification of urinary 8-hydroxy-2′-deoxyguanosine: measurement with gas chromatography-mass spectrometry after single solid-phase extraction. *Biochem J* 2004; **380**: 541–8.
18 Weimann A, Belling D, Poulsen HE. Quantification of 8-oxo-guanine and guanine as the nucleobase, nucleoside and deoxynucleoside forms in human urine by high-performance liquid chromatography-electrospray tandem mass spectrometry. *Nucl Acids Res* 2002; **30**: E7.
19 Wu LL, Chiou CC, Chang PY, Wu JT. Urinary 8-OHdG: a marker of oxidative stress to DNA and a risk factor for cancer, atherosclerosis and diabetics. *Clin Chim Acta* 2004; **339**: 1–9.
20 Loft S, Vistisen K, Ewertz M, Tjonneland A, Overvad K, Poulsen HE. Oxidative DNA damage estimated by 8-hydroxydeoxyguanosine excretion in humans: influence of smoking, gender and body mass index. *Carcinogenesis* 1992; **13**: 2241–7.
21 Gackowski D, Speina E, Zielinska M *et al*. Products of oxidative DNA damage and repair as possible biomarkers of susceptibility to lung cancer. *Cancer Res* 2003; **63**: 4899–902.
22 Shigenaga MK, Gimeno CJ, Ames BN. Urinary 8-hydroxy-2′-deoxyguanosine as a biological marker of in vivo oxidative DNA damage. *Proc Natl Acad Sci USA* 1989; **86**: 9697–701.
23 Gackowski D, Rozalski R, Roszkowski K, Jawien A, Foksinski M, Olinski R. 8-Oxo-7,8-dihydroguanine and 8-oxo-7,8-dihydro-2′-deoxyguanosine levels in human urine do not depend on diet. *Free Radic Res* 2001; **35**: 825–32.
24 Lunec J, Holloway KA, Cooke MS, Faux S, Griffiths HR, Evans MD. Urinary 8-oxo-2′-deoxyguanosine. redox regulation of DNA repair in vivo? *Free Radic Biol Med* 2002; **33**: 875–85.
25 Demple B, Harrison L. Repair of oxidative damage to DNA, enzymology and biology. *Annu Rev Biochem* 1994; **63**: 915–48.
26 Hazra TK, Izumi T, Maidt L, Floyd RA, Mitra S. The presence of two distinct 8-oxoguanine repair enzymes in human cells: their potential complementary roles in preventing mutation. *Nucl Acids Res* 1998; **26**: 5116–22.
27 Bessho T, Tano K, Kasai H, Ohtsuka E, Nishimura S. Evidence for two DNA repair enzymes for 8-hydroxyguanine (7,8-dihydro-8-oxoguanine) in human cells. *J Biol Chem* 1993; **268**: 19416–21.
28 Dianov G, Bischoff C, Piotrowski J, Bohr VA. Repair pathways for processing of 8-oxoguanine in DNA by mammalian cell extracts. *J Biol Chem* 1998; **273**: 33811–6.
29 Hayakawa H, Taketomi A, Sakumi K, Kuwano M, Sekiguchi M. Generation and elimination of 8-oxo-7,8-dihydro-2′-deoxyguanosine 5′-triphosphate, a mutagenic substrate for DNA synthesis, in human cells. *Biochemistry* 1995; **34**: 89–95.
30 Maki H, Sekiguchi M. MutT protein specifically hydrolyses a potent mutagenic substrate for DNA synthesis. *Nature* 1992; **355**: 273–5.
31 Cooke MS, Evans MD, Herbert KE, Lunec J. Urinary 8-oxo-2′-deoxyguanosine – source, significance and supplements. *Free Radic Res* 2000; **32**: 381–97.
32 Takeuchi T, Nakajima M, Morimoto K. Establishment of a human system that generates O2- and induces 8-hydroxydeoxyguanosine, typical of oxidative DNA damage, by a tumor promoter. *Cancer Res* 1994; **54**: 5837–40.
33 Takeuchi T, Nakajima M, Ohta Y, Mure K, Takeshita T, Morimoto K. Evaluation of 8-hydroxydeoxyguanosine, a typical oxidative DNA damage, in human leukocytes. *Carcinogenesis* 1994; **15**: 1519–23.
34 Loft S, Poulsen HE. Estimation of oxidative DNA damage in man from urinary excretion of repair products. *Acta Biochim Pol* 1998; **45**: 133–44.
35 Bergtold DS, Simic MG, Alessio H, Cutler RG. Urine biomarkers for oxidative DNA damage. In: Simic MG, Taylor KA, Ward JF, von Sontag C, eds. *Oxygen Radicals in Biology and Medicine*. New York: Plenum Press, 1988; 483–90.
36 Kasai H, Nishimura S. Hydroxylation of deoxyguanosine at the C-8 position by ascorbic acid and other reducing agents. *Nucl Acids Res* 1984; **12**: 2137–45.
37 Greenberg MM. In vitro and in vivo effects of oxidative damage to deoxyguanosine. *Biochem Soc Trans* 2004; **32**: 46–50.
38 Higuchi Y. Chromosomal DNA fragmentation in apoptosis and necrosis induced by oxidative stress. *Biochem Pharmacol* 2003; **66**: 1527–35.
39 Simon HU, Haj-Yehia A, Levi-Schaffer F. Role of reactive oxygen species (ROS) in apoptosis induction. *Apoptosis* 2000; **5**: 415–18.
40 Hengartner MO, Apoptosis. DNA, destroyers. *Nature* 2001; **412**: 27–9.
41 Davies AM, Hershman S, Stabley GJ, Hoek JB, Peterson J, Cahill A. A Ca^{2+}-induced mitochondrial permeability transition causes complete release of rat liver endonuclease G activity from its exclusive location within the mitochondrial intermembrane space. Identification of a novel endo-exonuclease activity residing within the mitochondrial matrix. *Nucl Acids Res* 2003; **31**: 1364–73.
42 Barry ME, Pinto-Gonzalez D, Orson FM, McKenzie GJ, Petry GR, Barry MA. Role of endogenous endonucleases and tissue site in transfection and CpG-mediated immune activation after naked DNA injection. *Hum Gene Ther* 1999; **10**: 2461–80.
43 Hibino Y, Iwakami N, Sugano N. A nuclease from rat-liver nuclei with endo- and exonucleolytic activity. *Biochim Biophys Acta* 1991; **1088**: 305–7.
44 Cordis GA, Goldblatt PJ, Deutscher MP. Purification and characterization of a major endonuclease from rat liver nuclei. *Biochemistry* 1975; **14**: 2596–603.

45 Toh Y, Yamamoto M, Endo H, Misumi Y, Ikehara Y. Isolation and characterization of a rat liver alkaline phosphatase gene. A single gene with two promoters. *Eur J Biochem* 1989; **182**: 231–7.
46 Alpers DH, Eliakim R, DeSchryver-Kecskemeti K. Secretion of hepatic and intestinal alkaline phosphatases: similarities and differences. *Clin Chim Acta* 1990; **186**: 211–23.
47 Yusifov TN, Abduragimov AR, Gasymov OK, Glasgow BJ. Endonuclease activity in lipocalins. *Biochem J* 2000; **347**: 815–19.
48 Pan CQ, Lazarus. RA. Hyperactivity of human DNase I variants. Dependence on the number of positively charged *residues and concentration*, length, and environment of DNA. *J Biol Chem* 1998; **273**: 11701–8.
49 Fraga CG, Shigenaga MK, Park JW, Degan P, Ames BN. Oxidative damage to DNA during aging. 8-hydroxy-2′-deoxyguanosine in rat organ DNA and urine. *Proc Natl Acad Sci USA* 1990; **87**: 4533–7.
50 Tchou J, Bodepudi V, Shibutani S, Antoshechkin I, Miller J, Grollman AP, Johnson F. Substrate specificity of Fpg protein. Recognition and cleavage of oxidatively damaged DNA. *J Biol Chem* 1994; **269**: 15318–24.
51 David SS, Williams SD. Chemistry of glycosylases and endonucleases involved in base-excision repair. *Chem Rev* 1998; **98**: 1221–62.
52 Weimann A, Riis B, Poulsen HE. Oligonucleotides in human urine do not contain 8-oxo-7,8-dihydrodeoxyguanosine. *Free Radic Biol Med* 2004; **36**: 1378–82.

 doi: 10.1111/j.1349-7006.2005.00004.x

Available online at www.sciencedirect.com
SCIENCE DIRECT®
Immunology Letters 95 (2004) 233–236
Immunology Letters
www.elsevier.com/locate/

Short communication

Oxidative damages in chronic inflammation of a mouse autoimmune disease model

Minyi Shi[a], Baohui Xu[a,b,*], Xin Wang[c], Kohji Aoyama[a], Sara A. Michie[b], Toru Takeuchi[a]

[a] *Department of Environmental Medicine, Faculty of Medicine, Kagoshima University, 8-35-1 Sakuragaoka, Kagoshima 890-8520, Japan*
[b] *Department of Pathology, Stanford University School of Medicine, CCSR Room 3240, 269 Campus Drive, Stanford, CA 94305-5324, USA*
[c] *Division of Antiviral Chemotherapy, Center for Chronic Viral Diseases, Faculty of Medicine, Kagoshima University, 8-35-1 Sakuragaoka, Kagoshima 890-8520, Japan*

Received 30 June 2004; received in revised form 6 July 2004; accepted 13 July 2004
Available online 6 August 2004

Abstract

Reactive oxygen species are generated in many types of inflammation; it is unclear, however, if inflammation leads to oxidative damage of DNA, proteins and lipids within the inflamed tissues. In this study, we used mice that are homozygous for the *alymphoplasia* (*aly*) mutation as a model to determine if inflammation induces oxidative damage in liver and pancreas. We found that 8-hydroxy-2'-deoxyguanosine (8OHdG), which is a product of oxidative DNA damage, increases with age in livers and pancreata of C57BL/6$^{aly/aly}$ (*aly/aly*) and C57BL/6 wild type (WT) mice. The 8OHdG levels in liver, but not in pancreas, of aged *aly/aly* mice were significantly higher than those in age-matched WT mice. We showed that aging enhances oxidative protein damage, as measured by carbonylated protein contents, in the pancreata of WT but not *aly/aly* mice. In contrast, neither aging nor inflammation was associated with lipid damage, as measured by thiobarbituric acid-reactive substances (TBARS), in *aly/aly* or WT mice. Our results indicate that chronic inflammation in liver but not pancreas leads to increased oxidative damage to DNA, but not to lipids and proteins in *aly/aly* mouse model.

Keywords: Oxidative damage; Inflammation; Mice

Reactive oxygen species (ROS) are continuously generated as a consequence of biophysical and pathological reactions and adequately removed by antioxidant systems. If ROS are overproduced and/or inadequately removed by antioxidant systems, they cause oxidative damage to cellular DNA, proteins and lipids, which are involved in a number of degenerative, neoplastic and immune or inflammatory disorders [1,2]. The generation of ROS is enhanced in various inflammatory diseases [3–5]; it is thus clear that inflammation potentially results in oxidative damage to DNA, lipids and proteins. Previous reports have mainly focused on the measurement of oxidative damages in serum, peripheral leukocytes and/or tumor tissues obtained from individuals with chronic inflammatory diseases [6–8], but information on oxidative damages at inflamed sites are very limited.

Mice that are homozygous for the alymphoplasia (*aly*) mutation develop autoimmune-mediated chronic inflammation in multiple organs with increasing age due to point mutation in NF-κB-inducing kinase [9,10]. Because liver and pancreas play critical roles in homeostasis, we used C57BL/6$^{aly/aly}$ (*aly/aly*) mice as an inflammation model to explore the relation of inflammation with oxidative damage to DNA, lipids and proteins in liver and pancreas.

Aly/aly and its wild type control (C57BL/6) mice were obtained from Japan Clea (Osaka, Japan) and housed in the Kagoshima University Experimental Animal Facility un-

* Corresponding author. Tel.: +1 650 724 6525; fax: +1 650 736 0073.
E-mail address: baohuixu@stanford.edu (B. Xu).

0165-2478/$ – see front matter © 2004 Elsevier B.V. All rights reserved.
doi:10.1016/j.imlet.2004.07.003

der specific pathogen-free conditions. Seven to nine young (10–11 weeks) or aged (56–60 weeks) mice, for each strain, were used in each experiment. Mice were sacrificed, and their livers and pancreata were immediately removed, frozen on dry ice, and stored at −80 °C for biochemical studies.

8-Hydroxy-2′-deoxyguanosine (8-OHdG) was used as oxidative DNA damage marker and was detected as described previously [11]. DNA was extracted by incubating tissue homogenates with proteinase K (50 units/ml, Applied Biosystems, Foster City, CA) at 60 °C for 2 h, precipitated with ethanol and then dissolved in distilled water. After being incubated with nuclease P1 (60 units/ml, Seikagaku Corporation, Tokyo, Japan) and alkaline phosphatase (6 units/ml, Sigma Chemical Co, St. Louis, MO, USA) sequentially, 8-OHdG and dG contents were then detected by HPLC with electrochemical and UV detectors (Coulochem II, ESA, Chelmsford, MA), respectively. Data are expressed as the molar ratio of 8-OHdG to 10^5 dG.

Protein carbonyl contents reflecting oxidative protein damage were detected as previously described [12]. Proteins were extracted from tissues in the presence of proteinase inhibitor cocktails (0.5 μg/ml aprotinin, 0.7 μg/ml pepstatin, 0.5 μg/ml leupeptin; Sigma) in phosphate buffer (pH 7.5). Samples were incubated on ice for 15 min, and centrifuged at 10,000 × *g* for 15 min. The supernatants containing 2–3 mg proteins were incubated with four volumes of 10 mM 2,4-dinitrophenylhydrazine (DNPH, Nacalai Tesque, Kyoto, Japan) in 2 M HCl at room temperature for 1 h in the dark. This resulted in the formation of 2,4-dinitrophenyl adducts on proteins by reacting protein carbonyl with DNPH. Proteins were precipitated with an equal volume of 20% and 10% TCA sequentially, washed with ethanol:ethyl acetate (1:1), and resuspended in 6 M guanidine hydrochloride (Nacalai Tesque) in 20 mM phosphate buffer/trifluoroacetic acid (pH 2.3) for spectrophotometric analysis. Carbonyl contents were calculated using a molar extinction coefficient of 22.0 mM^{-1} cm^{-1} and expressed as nmol carbonyl/mg protein.

In order to know how age and inflammation affect oxidative DNA damage, we compared 8-OHdG levels in the livers and pancreata of age-matched *aly/aly* and WT mice. As shown in Fig. 1, young *aly/aly* and WT mice had almost identical hepatic 8-OHdG levels. In *aly/aly* mice, there was a four-fold increase in liver 8-OHdG with aging (Fig. 1A; $P < 0.01$), while hepatic 8-OHdG levels of WT mice only increased 1.5-fold with aging (Fig. 1A; $P = 0.11$). Moreover, hepatic 8-OHdG levels of aged *aly/aly* mice were significantly higher than those of age-matched WT mice ($P < 0.01$). In pancreas, mean 8-OHdG levels in aged mice were approximately twice that in young mice for each genotype (Fig. 1B; $P < 0.05$ for WT mice, $P = 0.14$ for *aly/aly* mice). Although pancreatic 8-OHdG levels in aged *aly/aly* mice were higher than those of age-matched WT mice, the differences were not significant ($P = 0.29$).

Further, we examined how age and inflammation influence protein oxidative damage in livers and pancreata using protein carbonyl contents as a marker. As seen in Fig. 2,

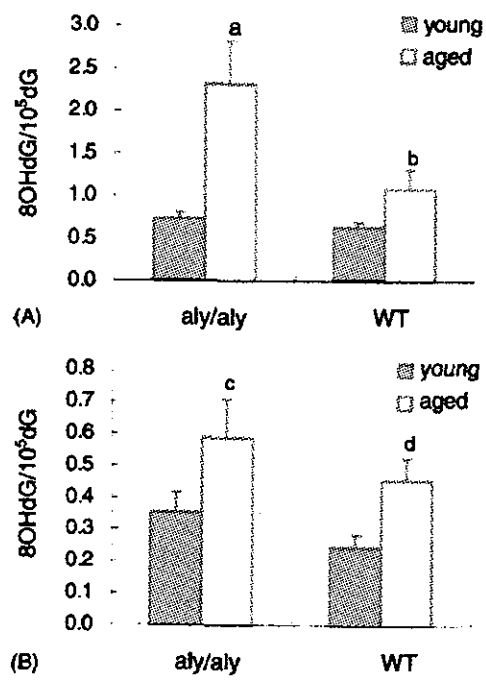

Fig. 1. Contents of 8-OHdG in DNA from the livers (A) and pancreata (B) of C57BL/6 *aly/aly* and WT mice. Aged mice: 56–60 weeks; young mice: 10–11 weeks. Data were obtained from seven to nine mice for each group and are represented as mean and standard error. Two-way analysis of variance was used to test for difference between groups. [a] $P < 0.05$ compared with both young *aly/aly* and aged WT mouse liver, [b] $P = 0.1148$ compared with young WT mouse liver, [c] $P = 0.1422$ compared with young *aly/aly* mouse pancreas, [d] $P < 0.05$ compared with young WT mouse pancreas.

hepatic carbonyl concentrations in aged *aly/aly* mice were virtually identical to those of aged WT mice (Fig. 2A). We did not find significant differences in hepatic carbonyl contents in young versus aged *aly/aly* mice, young versus aged WT mice, or young *aly/aly* versus young WT mice. In contrast to liver, carbonyl contents in the pancreata of aged WT mice were significantly higher than in pancreata of young WT mice (Fig. 2B, $P < 0.05$). However, pancreatic carbonyl concentrations in aged *aly/aly* mice were similar to those in young *aly/aly* mice. Unlike oxidative DNA damage in the livers, we did not observe significant differences in carbonyl levels in pancreas between aged *aly/aly* and WT mice.

This study showed a trend for age-dependent increases in oxidative damage to DNA in the liver and pancreas as measured by 8-OHdG level. Our results are in agreement with previous reports describing age-dependent increases in oxidative damage to DNA in multiple tissues including liver, kidney, brain, heart, intestine and pancreas [13,14]. Furthermore, we showed that oxidative damage to pancreatic proteins increased with increasing age only in WT whereas it was not seen in the livers of WT or *aly/aly* mice. In addition, analyzing oxidative lipid damage in the liver and pancreas using lipid peroxidation as a marker, we found that age did not cause lipid oxidative damage at our experimental settings (data not shown). These results support previous results that oxidative lipid and protein damages varied depending on

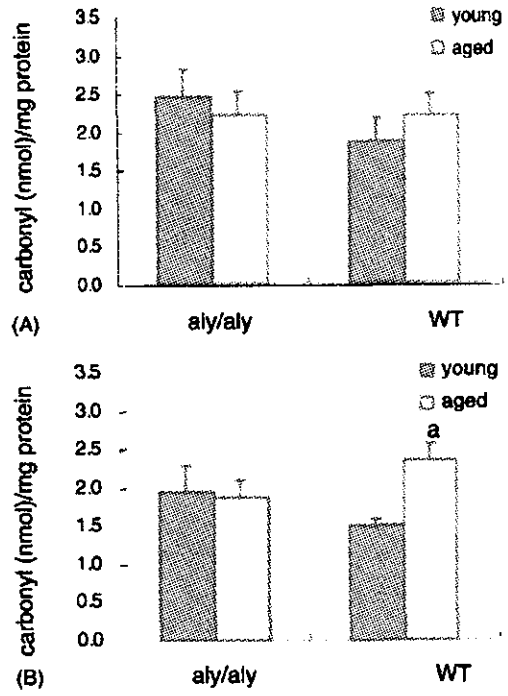

Fig. 2. Protein carbonyl contents in livers (A) and pancreata (B) of C57BL/6 *aly/aly* and WT mice. Data were obtained from seven to nine mice for each group and are represented as mean and standard error. Two-way analysis of variance was used to test for difference between groups. [a] $P < 0.05$ compared with young WT mice.

which tissues, cellular fractions and/or markers are examined [15–17].

More importantly, we found that 8-OHdG was highly accumulated only in inflamed livers of aged *aly/aly* mice but not in normal livers of aged WT mice. There was no significant correlation in 8-OHdG levels between liver and pancreas of *aly/aly* mice ($r = 0.25$, $P > 0.05$). These findings suggest that elevated 8-OHdG levels in inflamed livers of aged *aly/aly* mice are ascribed to liver inflammation but not to individual mouse variation. Previous studies have shown that oxidative DNA damage was usually accompanied by the damage to proteins and/or lipids in human inflamed liver diseases. For example, oxidative damages to DNA, lipids and proteins were seen in alcoholic liver disease [18]. Oxidative DNA damage coexisted with severe lipid damage in chronic hepatitis C more than in hepatitis B [19,20]. In our study, we did not find significant oxidative lipid and protein damages in the inflamed liver of aged *aly/aly* mice by measuring protein carbonyl contents and lipid peroxidation; our findings thus suggest that oxidative damage to DNA is more predominant than lipid and protein damages in inflamed livers of *aly/aly* mice.

High levels of ROS caused by their overproduction and/or failure to be removed by antioxidant enzymes lead to oxidative DNA damage. It has been shown that increasing age did not reduce antioxidant enzymes in mouse livers [13]. Inflammatory cells in the livers of aged *aly/aly* mice are mainly $CD4^+$ T cells [10]. Since T cells produce hydrogen peroxide and superoxide upon activation [4,21], ROS over-generated by infiltrated T cells may thus contribute to elevated 8-OHdG in the inflamed livers of aged *aly/aly* mice.

In summary, the present study showed that chronic inflammation in the livers, but not pancreata, of *aly/aly* mice led to elevated oxidative DNA damage without significant affects on lipids and proteins. It is thus possible that liver inflammation in aged *aly/aly* mice may be predisposed to tumorigenesis by enhancing 8-OHdG accumulation.

Acknowledgements

We thank Prof. Kanehisa Morimoto, Osaka University for his encouragement and Miss Chiko Yumiba, Kagoshima University for her administrative and technical assistance during this work. This work was supported by grants from the Japan Society for Science Promotion to BH Xu: C2-15590515 and T. Takeuchi: C2-12671664, and a Digestive Disease Center grant (DK56339) from the NIH.

References

[1] Cooke MS, Evans MD, Dizdaroglu M, Lunec J. Oxidative DNA damage: mechanisms, mutation, and disease. FASEB J 2003;17:1195–214.
[2] Floyd RA. Role of oxygen free radicals in carcinogenesis and brain ischemia. FASEB J 1990;4:2587–97.
[3] Bowler RP, Crapo JD. Oxidative stress in allergic respiratory diseases. J Allergy Clin Immunol 2002;110:349–56.
[4] MacMicking JD, Willenborg DO, Weidemann MJ, Rockett KA, Cowden WB. Elevated secretion of reactive nitrogen and oxygen intermediates by inflammatory leukocytes in hyperacute experimental autoimmune encephalomyelitis: enhancement by the soluble products of encephalitogenic T cells. J Exp Med 1992;176:303–7.
[5] Simmonds NJ, Allen RE, Stevens TR, Van Someren RN, Blake DR, Rampton DS. Chemiluminescence assay of mucosal reactive oxygen metabolites in inflammatory bowel disease. Gastroenterology 1992;103:186–96.
[6] Shimoda R, Nagashima M, Sakamoto M, Yamaguchi N, Hirohashi S, Yokota J, Kasai H. Increased formation of oxidative DNA damage, 8-hydroxydeoxyguanosine, in human livers with chronic hepatitis. Cancer Res 1994;54:3171–2.
[7] Dandona P, Thusu K, Cook S, Snyder B, Makowski J, Armstrong D, Nicotera T. Oxidative damage to DNA in diabetes mellitus. Lancet 1996;347:444–5.
[8] Bashir S, Harris G, Denman MA, Blake DR, Winyard PG. Oxidative DNA damage and cellular sensitivity to oxidative stress in human autoimmune diseases. Ann Rheum Dis 1993;52:659–66.
[9] Shinkura R, Kitada K, Matsuda F, Tashiro K, Ikuta K, Suzuki M, Kogishi K, Serikawa T, Honjo T. Alymphoplasia is caused by a point mutation in the mouse gene encoding Nf-kappa b-inducing kinase. Nat Genet 1999;22:74–7.
[10] Tsubata R, Tsubata T, Hiai H, Shinkura R, Matsumura R, Sumida T, Miyawaki S, Ishida H, Kumagai S, Nakao K, Honjo T. Autoimmune disease of exocrine organs in immunodeficient alymphoplasia mice: a spontaneous model for Sjogren's syndrome. Eur J Immunol 1996;26:2742–8.
[11] Nakajima M, Takeuchi T, Morimoto K. Determination of 8-hydroxydeoxyguanosine in human cells under oxygen-free conditions. Carcinogenesis 1996;17:787–91.

[12] Reznick AZ, Packer L. Oxidative damage to proteins: spectrophotometric method for carbonyl assay. Methods Enzymol 1994;233:357–63.
[13] Hamilton ML, Van Remmen H, Drake JA, Yang H, Guo ZM, Kewitt K, Walter CA, Richardson A. Does oxidative damage to DNA increase with age? Proc Natl Acad Sci USA 2001;98:10469–74.
[14] Fraga CG, Shigenaga MK, Park JW, Degan P, Ames BN. Oxidative damage to DNA during aging: 8-hydroxy-2′-deoxyguanosine in rat organ DNA and urine. Proc Natl Acad Sci USA 1990;87:4533–7.
[15] Davies SM, Poljak A, Duncan MW, Smythe GA, Murphy MP. Measurements of protein carbonyls, ortho- and meta-tyrosine and oxidative phosphorylation complex activity in mitochondria from young and old rats. Free Radic Biol Med 2001;31:181–90.
[16] Bejma J, Ramires P, Ji LL. Free radical generation and oxidative stress with ageing and exercise: differential effects in the myocardium and liver. Acta Physiol Scand 2000;169:343–51.
[17] Hayashi T, Miyazawa T. Age-associated oxidative damage in microsomal and plasma membrane lipids of rat hepatocytes. Mech Ageing Dev 1998;100:231–42.
[18] Seki S, Kitada T, Sakaguchi H, Nakatani K, Wakasa K. Pathological significance of oxidative cellular damage in human alcoholic liver disease. Histopathology 2003;42:365–71.
[19] Niemela O, Parkkila S, Britton RS, Brunt E, Janney C, Bacon B. Hepatic lipid peroxidation in hereditary hemochromatosis and alcoholic liver injury. J Lab Clin Med 1999;133:451–60.
[20] Kitada T, Seki S, Iwai S, Yamada T, Sakaguchi H, Wakasa K. In situ detection of oxidative DNA damage, 8-hydroxydeoxyguanosine, in chronic human liver disease. J Hepatol 2001;35:613–8.
[21] Devadas S, Zaritskaya L, Rhee SG, Oberley L, Williams MS. Discrete generation of superoxide and hydrogen peroxide by T cell receptor stimulation: selective regulation of mitogen-activated protein kinase activation and fas ligand expression. J Exp Med 2002;195:59–70.

Available online at www.sciencedirect.com
SCIENCE DIRECT®
Mutation Research 572 (2005) 132–141
Fundamental and Molecular Mechanisms of Mutagenesis
www.elsevier.com/locate/molmut
Community address: www.elsevier.com/locate/mutres

Frequent retention of heterozygosity for point mutations in *p53* and *Ikaros* in *N*-ethyl-*N*-nitrosourea-induced mouse thymic lymphomas

Shizuko Kakinuma[a,*], Mayumi Nishimura[a], Ayumi Kubo[a], Jun-ya Nagai[a], Yoshiko Amasaki[a], Hideyuki J. Majima[b], Toshihiko Sado[a], Yoshiya Shimada[a,**]

[a] *Low Dose Radiation Effect Research Project, National Institute of Radiological Sciences, Chiba, Japan*
[b] *Department of Oncology, Division of Maxillofacial Radiology and Department of Space Environmental Medicine, Graduate School of Medical and Dental Sciences, Kagoshima University, Kagoshima, Japan*

Received 19 September 2004; received in revised form 29 December 2004; accepted 7 January 2005

Abstract

In agreement with Knudson's two-hit theory, recent findings indicate that the inactivation of tumor suppressor genes is not only mediated by the loss of function but also by the dominant-negative or gain-of-function activity. The former generally accompanies loss of a wild-type allele whereas in the latter a wild-type allele is retained. *N*-Ethyl-*N*-nitrosourea (ENU), which efficiently induces point mutations, reportedly leads to the development of tumors by activating *ras* oncogenes. Little is known about how ENU affects tumor suppressor genes and, therefore, we examined ENU-induced mutations of *p53* and *Ikaros* in thymic lymphomas and compared these with mutations of K*ras*. In addition, loss of heterozygosity was examined for chromosome 11 to which both *p53* and *Ikaros* were mapped. The frequency of point mutations in *p53* and *Ikaros* was 30% (8/27) and 19% (5/27), respectively, comparable to that observed in K*ras* (33%: 9/27). In total, 14 of the 27 thymic lymphomas examined (52%) harbored mutations in at least one of these genes. One *Ikaros* mutation was located at the splice donor site, generating a novel splice isoform lacking zinc finger 3, *Ik (F3del)*. Interestingly, 90% (10/11) of the tumors with point mutations retained wild-type alleles of *p53* and *Ikaros*. Sequence analysis revealed that the most common nucleic acid substitutions were T > A (4/8) in *p53*, T > C (4/5) in *Ikaros* and G > A/T (8/9) in K*ras*, suggesting that the spectrum of mutations was gene dependent. These results suggest that point mutations in tumor suppressor genes without loss of the wild-type allele play an important role in ENU-induced lymphomagenesis.

Keywords: ENU; Heterozygous mutation; *p53*; *Ikaros*

1. Introduction

Tumor suppressor gene function can be inactivated either by point mutations or by deletion of both the alleles, known as Knudson's "two-hit" hypothesis [1,2]. In

* Corresponding author. Tel.: +81 34 206 3221; fax: +81 34 206 4138.
** Co-corresponding author.
E-mail addresses: skakinum@nirs.go.jp (S. Kakinuma), y_shimad@nirs.go.jp (Y. Shimada).

0027-5107/$ – see front matter © 2005 Elsevier B.V. All rights reserved.
doi:10.1016/j.mrfmmm.2005.01.010

an examination of colon cancers, Vogelstein and colleagues found that the most prevalent pattern of *p53* mutations was a point mutation in one allele concomitant with the loss of the other allele [3]. On the other hand, several lines of evidence suggest that given types of p53 act as oncogenes in a dominant manner in the presence of a wild-type allele [3,4]. Since p53 functions as a tetrameric transcription factor, mutant p53 lacking DNA-binding ability is thought to inhibit the function of wild-type p53 [5,6]. These lines of evidence indicate that negative dominancy adds a new perspective to our understanding of tumor suppressors. However, little data are available on oncogenic changes in other tumor suppressor genes.

Ikaros is a tumor suppressor gene for T and B cell leukemogenesis in both the mice and humans [7–10]. Ikaros is a Kruppel-type zinc finger transcription factor involved in lineage commitment and differentiation in the lymphoid cells. Heterozygous mice expressing a short Ikaros isoform lacking the DNA-binding zinc fingers show aberrant T cell differentiation and develop thymic lymphomas within 3 months after birth [11]. Biochemical analysis has revealed that Ikaros forms homodimers or heterodimers with other Ikaros family members such as Aiolos or Helios [12,13]. Thus, short Ikaros isoforms lacking DNA-binding domains function in a dominant-negative fashion against wild-type Ikaros. Similar to p53, one might predict that Ikaros mutants containing lesions in the DNA-binding domain would affect wild-type Ikaros in a dominant-negative manner. We previously demonstrated that short Ikaros isoforms lacking the DNA-binding domain are expressed in radiation-induced mouse thymic lymphomas [14,15]. These lymphomas frequently retain a wild-type allele, suggesting dominant-negative interactions. Point mutations of *Ikaros* were observed in other lymphomas that had lost a wild-type allele, consistent with Knudson's two-hit theory [14–17].

N-Ethyl-*N*-nitrosourea (ENU) is a hyper-mutable alkylating agent that efficiently induces point mutations [18,19]. Treatment of mice with ENU leads to a high incidence of thymic lymphoma. Mutation of *Kras* genes is more frequently observed in ENU-induced lymphomas than in radiation-induced lymphomas, suggesting that oncogene activation plays an important role in ENU-induced lymphomagenesis [20–23]. In contrast, a genome-wide survey of loss of heterozygosity (LOH) showed a significantly lower LOH rate in ENU-induced lymphomas than in radiation-induced lymphomas [14]. ENU also induces point mutations within the *Aprt* locus but these lesions do not occur by deletion/recombination [24,25]. Therefore, it is less likely that inactivation of tumor suppressor genes contributes to ENU-induced lymphomagenesis. As mentioned above, however, point mutations of *p53* without accompanying LOH have occasionally been reported [3].

The aim of this study was to examine the rate and spectrum of mutations in *Ikaros* and *p53* tumor suppressor genes associated with LOH and to determine the contribution of tumor suppressor genes to ENU-induced tumorigenesis. We found that the mutation rates of *Ikaros* and *p53* are comparable to that of *Kras* and that, in contrast to radiation-induced lymphomas, ENU-induced lymphomas retain a wild-type allele of these genes. Thus, we conclude that heterozygous point mutations of tumor suppressor genes significantly contribute to ENU-induced lymphomagenesis.

2. Materials and methods

2.1. Mice and tumor induction

B6C3F1 mice were purchased from Charles River, Kanagawa, Japan. Induction of thymic lymphomas by ENU (Nakali, Japan) was as described previously [26]. Briefly, thymic lymphomas were induced in female mice that were a cross between thymic lymphoma-susceptible C57BL/6 and thymic lymphoma-resistant C3H strains. Five-week-old mice received 400 ppm ENU in their drinking water for 8 weeks. Mice were observed daily until moribund after which they were sacrificed under ether anesthesia and autopsied. Thymic tissue was then removed, weighed and prepared for serological and molecular analyses [15]. All the animal experiments were conducted in compliance with the institutional guidelines for the care of laboratory animals.

2.2. Antibodies and immunofluorescence analysis

FITC-conjugated anti-CD8, anti-cKit, anti-CD44, and anti-TCRαβ, and PE-conjugated anti-CD4, anti-IL2, anti-CD3, and anti-TCRγδ were purchased from Pharmingen (San Diego, CA). After dispersing

the thymus until single cells were obtained, 10^6 cells were resuspended in 50 μl PBS supplemented with 1% FBS and FITC and/or PE-conjugated antibodies at an optimal dilution for 30 min on ice. Control levels of fluorescence were determined after staining with the appropriate isotype-specific Igs. The relative fluorescence intensity of 10,000 cells in each sample was measured using FACScan and was analyzed with Cell Quest software (Becton Dickinson, Mountain View, CA).

2.3. Western blot analysis of p53 and Ikaros in thymocytes

Western blotting was performed as described previously [15] with the following minor modifications: after transfer of proteins from the gel, the membrane was blocked and probed with polyclonal antisera against p53 (1:5000; Santa Cruz Biotechnology Inc., Santa Cruz, CA) or Ikaros (1:5000). Blots were washed and then incubated with a peroxidase-conjugated goat anti-rabbit IgG secondary antibody (1:50,000; Amersham Pharmacia Biotech Inc., Piscataway, NJ). Ikaros proteins were detected using Super Signal Dura Chemiluminescent Substrate (Pierce, Rockford, IL) and were analyzed using a Kodak Digital analyzer (Kodak, Rochester, NY).

2.4. LOH analysis

Genomic DNA was extracted from the tumors according to the standard techniques. The LOH region on chromosome 11 was defined using the following 10 polymorphic loci: *D11Mit71*, *D11Mit62*, *D11Mit2*, *D11Mit204*, *D11Mit150*, *D11Mit77*, *D11Mit20*, *Acrb*, *D11Mit14* and *D11Mit203*. Single-strand length polymorphism (SSLP) analysis was performed as previously described [14].

2.5. Mutation analysis of Ikaros, p53 and Kras

Total RNA extracted from lymphoma cells was reverse-transcribed to obtain cDNA as described previously [15]. Expression status of *Ikaros* was determined using the primers *Ikaros* 2F and 7R and *Gapd* (sense and antisense) as a control. Mutations in the genes *p53*, *Ikaros* and *Kras* were assessed in all thymic lymphomas. The primer sets for the amplification of the entire *Ikaros* cDNA (exons 1–7) were *Ikaros* 1F and 7R(3) [15]. Sequencing to determine mutations in the splicing junction between exons 3 and 4, or exons 4 and 5 was performed using PCR fragments amplified from genomic DNA using LA Taq (Takara Shuzo Co., Shiga, Japan). The primer set for the junction between exons 3 and 4 was sense 3F(2), 5′-AGG CAT TCG ACT TCC TAA CG-3′ and antisense 4R, 5′-GGT TGC ACT GGA AAG GCC GT-3′. The primer set for the junction between exons 4 and 5 was sense 4F, 5′-GGT GAA CGG CCT TTC CAG TGC-3′ and antisense 5R, 5′-TGT TTA TAG CTC CGG CCA CAA T-3′. PCR products were purified using Quantum Prep Freeze N Squeeze DNA extraction spin columns (Bio-Rad, Hercules, CA), concentrated by ethanol precipitation and suspended in distilled water prior to sequencing. The primer set for the amplification of *p53* cDNA (between exons 5 and 9 containing the DNA-binding domain) was sense *p53* F(1), 5′-CCC TGT CAT CTT TTG TCC CTT-3′ and antisense *p53* R(1), 5′-CGC GGA TCT TGA GGG TGA AAT-3′. For the *ras* gene, the first, second and third exons of K*ras* were analyzed by single-strand conformation polymorphism (SSCP) analysis of genomic DNA followed by TA-cloning sequencing as described previously [27].

Sequencing was performed using the BigDye Terminator Cycle Sequencing FS Ready Reaction kit for both the direct and TA-cloning sequencing (PE Applied Biosystems, Foster City, CA) and the products were analyzed on an ABI PRISM 310 DNA Sequencer (PE Applied Biosystems). For direct sequencing, at a minimum, both forward and reverse sequences were determined for each sample. For TA-cloning, at least five clones from each sample were analyzed. Any mutations detected in cDNA were confirmed by analysis of the corresponding genomic DNA to exclude the possibility of false positives resulting from the errors during PCR amplification.

3. Results

3.1. Development of thymic lymphomas and phenotypic staging

Five-week-old mice were treated with ENU for 8 weeks. Thymic lymphomas developed in 75% (45/60) of the mice. The average latency period was 7 ± 4 weeks after the end of the treatment and the lifes-

pan of treated mice was 20 ± 4 weeks. These values are much shorter than those observed for lymphomas induced by X-irradiation (latency, 16 ± 3 weeks after treatment; lifespan, 22 ± 3 weeks) ($p < 0.01$) [14]. The mass of ENU-induced thymic lymphomas was 520 ± 34 mg compared with 486 ± 36 mg for X-ray-induced tumors (not significantly different; $p = 0.12$).

Expression of the surface antigens CD4, CD8, CD3, CD125 (IL2Rα), CD44, c-Kit, TCRαβ and TCRγδ was examined to classify the thymic lymphomas into stages of differentiation. Sixteen of the 19 thymic lymphomas (84%) were $CD4^+CD8^+$, 9 of which were immature $CD3^-$ with the remaining 7 being mature $CD3^+$. One thymic lymphoma was $CD4^+CD8^{\pm}CD3^+$, reflecting the mature differentiated stage of the $CD4^+$ single positive. The remaining two lymphomas were $CD4^{\pm}CD8^+CD3^-$ and $CD4^{\pm}CD8^-CD3^-$, both of which were at an immature stage. Expression of c-Kit and TCRγδ were negative in all the thymic lymphomas examined (data not shown). These results are consistent with the previous studies [21,28].

3.2. LOH status in chromosome 11

p53 and *Ikaros* are located on chromosome 11 in the telomeric (39.0 cM) and centromeric regions (6.0 cM), respectively. Ten microsatellite markers on chromosome 11 were used for allotyping in 27 thymic lymphomas. *p53* has been mapped close to *Acrb* and *Ikaros* has been mapped between *D11Mit62* and *D11Mit2* [14]. LOH was detected in 2/27 lymphomas (7%). These two tumors (S1603 and S1610) exhibited LOH at all loci examined, indicating non-disjunction as a mechanism of LOH. Thus, the frequency of LOH was low in ENU-induced thymic lymphomas compared with the LOH rates observed in radiation- (50%) or 1,3-butadiene-induced lymphomas (26%) [14,29].

3.3. Expression of Ikaros

We previously demonstrated that 25% of the radiation-induced thymic lymphomas from B6C3F1 mice have altered *Ikaros* expression (i.e., silencing or alternative splicing) [15]. The *Ikaros* expression pattern in ENU-induced lymphomas was essentially identical to that in the normal thymocytes (Fig. 1a), with concomitant expression of 750 and 490-bp products corresponding to *Ik1* and *Ik2*, respectively [30]. One

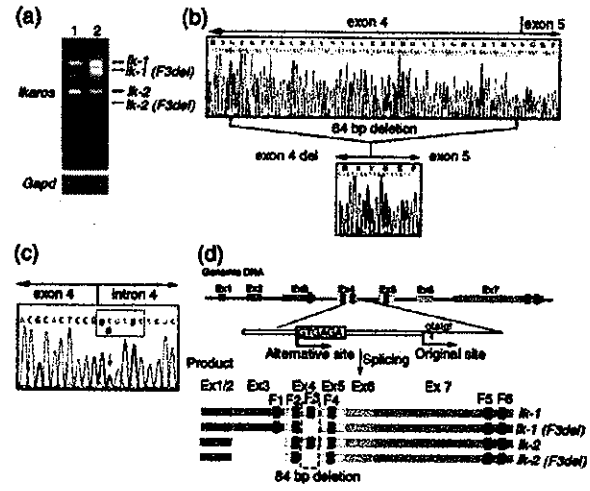

Fig. 1. Expression and sequence analysis of the shortened *Ikaros* isoform in ENU-induced thymic lymphoma S1624. (a) RT-PCR analysis of *Ikaros* expression in normal thymocytes from 6-week-old mice (lane 1) or in the thymic lymphoma S1624 (lane 2). Each cDNA sample was amplified with the primers for *Ikaros* (2F/7R) and *Gapd* (control). (b) Sequence analysis of *Ikaros* expressed in S1624. The upper panel depicts the sequence between exons 4 and 5 in *Ik1* or *Ik2* and the lower panel shows the sequence of the corresponding shortened fragment in S1624. Codons and amino acid sequences are shown above each sequence panel. An 84-bp deletion was found at the 3′ end of exon 4. (c) Heterozygous (t>t/g) point mutation in a splice donor site in intron 4 of S1624, as determined by direct sequencing. (d) Schematic presentation of genomic mutations and alternative splicing of *Ikaros* in S1624. A heterozygous mutation in intron 4 resulted in the creation of the mutant Ikaros isoforms *Ik-1 (F3del)* and *Ik-2 (F3del)* in addition to *Ik1* and *Ik2*.

lymphoma, S1624, expressed two additional isoforms of slightly reduced size relative to *Ik1* and *Ik2* (Fig. 1a). These results were confirmed by Western blotting (data not shown). Sequence analysis demonstrated that the shorter isoforms had an 84-bp deletion in the latter half of exon 4, resulting in the deletion of zinc-finger 3 within the N-terminal DNA-binding domain (Fig. 1b and d). We designated these internally deleted genes as *Ik1 (F3del)* and *Ik2 (F3del)*. No such *Ikaros* mutants have been reported previously. Cobb et al. [31] reported a deletion construct of *Ikaros dF3*, which is identical to *Ik (F3del)*, and showed loss of both DNA-binding activity and pericentromeric targeting ability in 3T3 fibroblasts.

We subsequently analyzed the genomic DNA sequence of the S1624 lymphoma between exons 4 and 5 of the *Ikaros* gene and identified a point mutation in

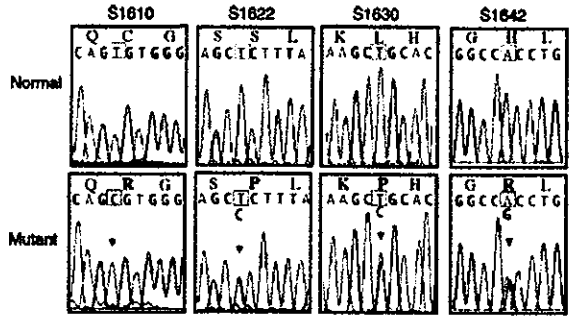

Fig. 2. Point mutations of *Ikaros* in ENU-induced thymic lymphomas. Each panel indicates codons and amino acid sequence for *Ikaros* (GenBank accession no. L03547 with insertion of exon 3) or mutants thereof. Arrows indicate the positions of base substitutions. The point mutation of S1610 (column 1) is homozygous while those of S1622 (column 2), S1630 (column 3) or S1642 (column 4) are heterozygous.

the splicing donor site within intron 4 (gtatgt > ggtatgt, Fig. 1c) that could potentially compromise donor function during pre-mRNA splicing. Consequently, the sequence GTGAGA in exon 4, located 84-bp upstream of the original splice donor site, was used as an altered (and novel) splice site. Because the point mutation was heterozygous, the wild-type allele underwent normal splicing as well. As a result, the S1624 lymphoma expressed the four alternative mRNAs *Ik1*, *Ik2*, *Ik1 (F3del)* and *Ik2 (F3del)* (Fig. 1d). This contrasts with the previous data in which no splice site mutations were found in the mouse thymic lymphomas and human leukemic cells expressing Ikaros isoforms *Ik4*, *Ik4 (del)*, *Ik6*, *Ik8* and *Ik8 (del)* [9,15].

3.4. Point mutations of Ikaros

Point mutations of *Ikaros* have also been described in radiation- and 1,2-butadiene-induced thymic lymphomas [15,17,29]. Therefore, we examined *Ikaros* mutations in 26 ENU-induced thymic lymphomas. Sequence analysis of the entire *Ikaros* cDNA (exons 1–7) and the corresponding genomic DNA revealed point mutations in four thymic lymphomas (S1610, S1622, S1630, S1642; Fig. 2; Table 1). Three of them (S1622, S1630, S1643) were heterozygous at the mutation site. All four were the missense mutations in the N-terminal zinc finger DNA-binding domain. Three of the four mutations (S1610, S1630, S1642) were located in the C_2H_2 zinc-finger structure important for interaction with zinc and one (S1622) was located at a serine residue next to leucine, which is a conserved hydrophobic residue within an α-helix involved in zinc finger secondary structure. The distribution of the point mutations was distinct from that seen in radiation-induced lymphomas where mutations were more sparsely distributed and were accompanied by LOH [15]. All point mutations were T > C transitions.

3.5. Analysis of p53 mutations

Next, we analyzed thymic lymphoma samples for the mutations in *p53*. Eight tumors (S1594, S1607, S1610, S1633, S1634, S1641, S1642 and S1643) harbored missense mutations in the DNA-binding region (Table 1). Two tumors (S1607 and S1610) did not express p53 protein while the other six (S1594, S1633, S1634, S1641, S1642 and S1643) expressed high levels of p53 (data not shown). These results are consistent with a previous report that mutant p53 has an increased half-life and accumulates in the nucleus [32]. As was the case for *Ikaros*, the majority (88%, 7/8) of lymphomas with *p53* point mutations retained a wild-type *p53* allele except for S1610.

3.6. Point mutations of Kras

3.6. Point mutations of Kras

Frequent mutations of the K*ras* oncogene have been reported in nitroso compound-induced tumors [21,33]. Seven tumors (S1601, S1607, S1622, S1630, S1631, S1634 and S1644) had K*ras* gene mutations, five of which (S1607, S1622, S1630, S1631, and S1644) were in codon 12, one (S1634) in codon 59 and one (S1601) in codon 61. All K*ras* mutations were heterozygous and retained a wild-type allele. Two tumors (S1607 and S1622) harbored two mutations concomitantly, displaying two additional bands in SSCP analysis (Fig. 3a), that resulted in nine point mutations in total. Sequence analysis after TA-cloning of the K*ras* gene revealed that these lymphomas contained three types of sequence in codon 12, namely GGT (wild-type), GAT and TGT, at a ratio of 3:2:5 (Fig. 3b).

3.7. Mutation spectrum in ENU-induced thymic lymphomas

The mutation and LOH status for each ENU-induced thymic lymphoma is summarized in Table 1.

Table 1
Alteration of *p53*, *Ikaros* and *Kras* and LOH status of chromosome 11 in ENU-induced thymic lymphomas (TL)

Sample	Latency (days)	TL size (mg)	*Ikaros*				*P53*				*Kras*	
			Codon	Nucleotide (aa)	Location	LOH[a]	Codon	Nucleotide (aa)	Protein[b]	LOH[a]	Codon	Nucleotide (aa)
S1594	110	743				–	160	TAC>CAC (Y>H)	+	–		
S1601	117	ND[c]				–				–	61	CAA>CTA (Q>L)
S1607	121	345				–	210	CGC>TGC (R>C)	–	–	12	GGT>TGT (G>C)
												GGT>GAT (G>D)
S1610	122	431	150	TGT>CGT (C>R)	F2[d]	B	213	GTG>TTG (V>L)	–	B		
S1622	130	864	215	TCT>CCT (S>P)	F4[e]	–				–	12	GGT>TGT (G>C)
											12	GGT>GAT (G>D)
S1624	130	615	int4+2	gt>gg (del 169–196)	F3del[f]	–				–		
S1630	132	994	166	CTG>CCG (L>P)	F2[d]	–				–	12	GGT>TGT (G>C)
S1631	136	309				–				–	12	GGT>GAT (G>D)
S1633	136	595				–	213	GTG>ATG (V>M)	+	–		
S1634	139	577				–	243	ATG>AAG (M>K)	+	–	59	GCA>GAA (A>E)
S1641	143	818				–	243	ATG>AAG (M>K)	+	–		
S1642	145	711	191	CAC>CGC (H>R)	F3[d]	–	190	CAT>CTT (H>L)	+	–		
S1643	145	892				–	194	GTG>GAG (V>E)	+	–		
S1644	145	877				–				–	12	GGT>GAT (G>D)

[a] Lost allele: B, B6; (–), heterozygous.
[b] Expression status of p53 protein: (+), over-expression; (–), no expression (normal type).
[c] ND: not determined.
[d] Mutation was located in the C_2H_2 zinc-finger structure for interaction with zinc.
[e] Mutation was located in an α-helix structure in the zinc-finger protein.
[f] Described in Fig. 1.

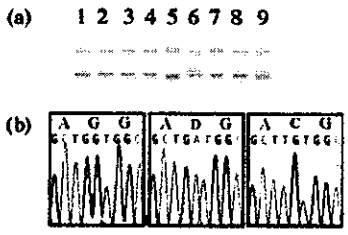

Fig. 3. Detection of *Kras* mutations in ENU-induced thymic lymphomas. (a) PCR-SSCP analysis. Lane 1 shows the *Kras* pattern from normal thymocytes, and lanes 2, 3, 4, 7 and 8 represent thymocytes from thymic lymphomas without *Kras* mutations. Lanes 5 (S1631), 6 (S1630) and 9 (S1607) show altered patterns. (b) Sequence analysis after TA-cloning of S1607 (lane 9 in panel a). Three types of sequence, GGT, GAT and TGT, were found at codon 12 (panel b).

In *Ikaros*, four of the five mutations (80%) were T > C. In *p53*, four of the eight mutations (50%) were T > A and two were G > A (25%). In *Kras*, four of the nine mutations were G > A (44%) and another four were G > T (44%). These results are in good agreement with the evidence that ENU produces significant levels of alkylation at oxygen atoms such as the O^6 position of guanine and the O^4 position of thymine in DNA [18]. The results also indicate, however, that the spectrum of base substitutions is different among these genes.

It is also noteworthy that 43% (6/14) of the lymphomas harbored double mutations. S1610 and S1642 harbored mutations in both *Ikaros* and *p53*. S1607 and S1634 had mutations in *p53* and *Kras*. S1622 and S1630 had mutations in *Ikaros* and *Kras*. In all, 14 of the 27 lymphomas (52%) had mutations in at least one of the three genes examined and most of these lymphomas also retained a wild-type allele of the *p53*, *Ikaros* and *Kras* genes.

4. Discussion

This study revealed point mutations in the tumor suppressor genes *p53* and *Ikaros* in 8 (30%) and 5 (19%) of the 27 ENU-induced thymic lymphomas, respectively. This was often accompanied by the retention of a wild-type allele (in 7/8 [88%] of *p53* mutations and 4/5 [80%] of *Ikaros* mutations). One of the *Ikaros* mutations was located at the splice donor site, generating a novel splice isoform lacking zinc finger 3, *Ik (F3del)*. Together with 7 lymphomas with *Kras* oncogene mutations (23%), 14 of the 27 (52%) thymic lymphomas harbored point mutations in at least 1 of the 3 genes examined.

Tumor suppressor genes can be inactivated by point mutations or deletions according to Knudson's "two-hit" hypothesis [1]. However, some tumor suppressor genes with particular types of mutations act as oncogenes in a dominant manner, probably by forming oligomeric complexes with wild-type or other proteins that results in the loss of wild-type protein function [5,34]. Recently, mice were produced having targeted point mutations of *p53* [35,36]. Mice heterozygous for a mutation in codon 172, R172H differed from p53+/− mice in tumor spectrum and metastatic frequency. Interestingly, loss of a wild-type *p53* allele was rarely observed in the tumors [35]. Cells from two other mice heterozygous for *p53* point mutations, R270H and P275S, exhibited delayed transcriptional activation of *p53* downstream target genes upon exposure to gamma-rays. They also showed severe defects in p53-dependent apoptosis, supporting negative dominance over wild-type p53 [36].

A *Plastic* mouse strain was recently developed that has the same point mutation as *Ikaros*, H191R, found in lymphoma S1642 (Fig. 2). It has been demonstrated that mice heterozygous for H191R, $Ikaros^{Plastic/+}$, develop leukemia/lymphomas frequently within 4 months after birth [37]. Although the lymphomas developed in $Ikaros^{Plastic/+}$ have not been examined for the loss of wild-type alleles, the S1642 lymphoma in the present study showed retention of a wild-type *Ikaros* allele. These data suggest negative dominance of this *Ikaros* point mutation in vivo. However, functional studies are required to confirm that this is indeed the case. There are other reports of tumor suppressor genes that are exceptions to the classical version of Knudson's two-hit theory [38,39]. These include *Caveolin-1* and *Smad4*. A point mutation, P132L, in codon 132 of *Caveolin-1* has been reported in 16% of the primary human breast cancers but no loss of heterozygosity of the wild-type *Caveolin-1* gene was observed [40]. A point mutation in *Smad4* has been frequently observed in pancreatic and colon cancers. Expression of Smad4 carrying an R497H mutation antagonized TGF-β signaling in a dominant-negative manner [41], consistent with the clinical observations that only one *Smad4* allele is affected in some cancers [42]. It seems likely that the cancers harboring heterozygous point mutations of Caveolin-1 and Smad4 are inactive for wild-type cave-

olin and Smad4 function because both Caveolin-1 and Smad4 form homo- and heteromeric complexes, respectively.

One cannot exclude the possibility, however, that inactivating one *p53* allele through the mutation results in a cellular phenotype caused by gene dosage reduction, a phenomenon previously described by others in p53+/– knockout mice [43]. Indeed, LOH at both *p53* and *Ikaros* loci without an additional point mutation in the other allele was found in lymphoma S1603. In addition, the p53 mutations found in the ENU-induced lymphomas are not the well known hot-spot mutations frequently found in the other tumor types that were previously shown to display dominant-negative activity [36,44]. These lines of evidence indicate that carcinogenesis occurs despite the production of wild-type tumor suppressor proteins in contrast to the standard definition of tumor suppressor genes.

In addition to the point mutations, alternative use of transcriptional initiation sites or alternative splicing that results in a lack of DNA-binding or transactivation activity may be another mechanism(s) to generate dominant-negative tumor suppressor proteins. N-terminally truncated p73 and several Ikaros isoforms (Ik4, Ik6 and Ik8) lacking DNA-binding domains have been reported in some tumors [12,45]. We previously reported that lymphomas expressing Ikaros splice variants (Ik4, Ik6 and Ik8) retain a wild-type *Ikaros* allele [15]. In the present study, lymphoma S1624 expressed a novel Ik (F3del) isoform caused by a point mutation at the splice site but retained a wild-type allele.

Knudson's two-hit model of tumor suppressor genes supposes biallelic disruption which frequently involves loss of a wild-type allele via deletion and/or mitotic recombination. LOH has previously been useful for predicting tumor suppressor loci. However, a growing number of reports have described candidate tumor suppressors that do not conform to this standard definition. These include loci that exhibit negative dominancy and haploinsufficiency. Indeed, we demonstrated here that lymphomas induced by ENU, which is effective at inducing point mutations but not in deletion and/or recombination events, frequently harbored mutations of tumor suppressor genes such as *p53* and *Ikaros* without accompanying LOH. Therefore, to obtain a more complete picture of carcinogenesis, it will be important to examine mutations/alterations of other tumor suppressor genes whose loci do not demonstrate LOH.

In summary, our data suggest that ENU facilitates T cell lymphomagenesis by dominant-negative inactivation of tumor suppressor gene function as well as by oncogene (*ras*) activation.

Acknowledgments

We thank Ms. E. Obara, Ms. M. Takada and Ms. K. Yajima for technical assistance, and the Division of Animal Facility staff for help with the laboratory analysis and maintenance of animals. We also thank Dr. T. Ogiu for his encouragement throughout the course of our research. This study was supported partly through a grant of "Ground-based Research Announcement for Space Utilization" promoted by the Japan Space Forum, and a grant of Long-rang Research Initiative (LRI) by Japan Chemical Industry Association (JCIA).

References

[1] A.G. Knudson Jr., Mutation and cancer: statistical study of retinoblastoma, Proc. Natl. Acad. Sci. U.S.A. 68 (1971) 820–823.
[2] A.G. Knudson, Antioncogenes and human cancer, Proc. Natl. Acad. Sci. U.S.A. 90 (1993) 10914–10921.
[3] J.M. Nigro, S.J. Baker, A.C. Preisinger, J.M. Jessup, R. Hostetter, K. Cleary, S.H. Bigner, N. Davidson, S. Baylin, P. Devilee, et al., Mutations in the *p53* gene occur in diverse human tumour types, Nature 342 (1989) 705–708.
[4] R. Mazars, L. Spinardi, M. BenCheikh, J. Simony-Lafontaine, P. Jeanteur, C. Theillet, p53 mutations occur in aggressive breast cancer, Cancer Res. 52 (1992) 3918–3923.
[5] P. Wang, M. Reed, Y. Wang, G. Mayr, J.E. Stenger, M.E. Anderson, J.F. Schwedes, P. Tegtmeyer, p53 domains: structure, oligomerization, and transformation, Mol. Cell. Biol. 14 (1994) 5182–5191.
[6] K.G. McLure, P.W. Lee, How p53 binds DNA as a tetramer, EMBO J. 17 (1998) 3342–3350.
[7] L. Sun, N. Heerema, L. Crotty, X. Wu, C. Navara, A. Vassilev, M. Sensel, G.H. Reaman, F.M. Uckun, Expression of dominant-negative and mutant isoforms of the antileukemic transcription factor Ikaros in infant acute lymphoblastic leukemia, Proc. Natl. Acad. Sci. U.S.A. 96 (1999) 680–685.
[8] L. Sun, M.L. Crotty, M. Sensel, H. Sather, C. Navara, J. Nachman, P.G. Steinherz, P.S. Gaynon, N. Seibel, C. Mao, A. Vassilev, G.H. Reaman, F.M. Uckun, Expression of dominant-negative Ikaros isoforms in T-cell acute lymphoblastic leukemia, Clin. Cancer Res. 5 (1999) 2112–2120.
[9] L. Sun, P.A. Goodman, C.M. Wood, M.L. Crotty, M. Sensel, H. Sather, C. Navara, J. Nachman, P.G. Steinherz, P.S. Gaynon, N. Seibel, A. Vassilev, B.D. Juran, G.H. Reaman, F.M. Uckun,

Expression of aberrantly spliced oncogenic Ikaros isoforms in childhood acute lymphoblastic leukemia, J. Clin. Oncol. 17 (1999) 3753–3766, see comments.

[10] H. Nakayama, F. Ishimaru, N. Avitahl, N. Sezaki, N. Fujii, K. Nakase, Y. Ninomiya, A. Harashima, J. Minowada, J. Tsuchiyama, K. Imajoh, T. Tsubota, S. Fukuda, T. Sezaki, K. Kojima, M. Hara, H. Takimoto, S. Yorimitsu, I. Takahashi, A. Miyata, S. Taniguchi, Y. Tokunaga, H. Gondo, Y. Niho, M. Harada, et al., Decreases in Ikaros activity correlate with blast crisis in patients with chronic myelogenous leukemia, Cancer Res. 59 (1999) 3931–3934.

[11] S. Winandy, P. Wu, K. Georgopoulos, A dominant mutation in the *Ikaros* gene leads to rapid development of leukemia and lymphoma, Cell 83 (1995) 289–299.

[12] L. Sun, A. Liu, K. Georgopoulos, Zinc finger-mediated protein interactions modulate Ikaros activity, a molecular control of lymphocyte development, EMBO J. 15 (1996) 5358–5369.

[13] B. Morgan, L. Sun, N. Avitahl, K. Andrikopoulos, T. Ikeda, E. Gonzales, P. Wu, S. Neben, K. Georgopoulos, Aiolos, a lymphoid restricted transcription factor that interacts with Ikaros to regulate lymphocyte differentiation, EMBO J. 16 (1997) 2004–2013.

[14] Y. Shimada, M. Nishimura, S. Kakinuma, M. Okumoto, T. Shiroishi, K.H. Clifton, S. Wakana, Radiation-associated loss of heterozygosity at the Znfn1a1 (Ikaros) locus on chromosome 11 in murine thymic lymphomas, Radiat. Res. 154 (2000) 293–300.

[15] S. Kakinuma, M. Nishimura, S. Sasanuma, K. Mita, G. Suzuki, Y. Katsura, T. Sado, Y. Shimada, Spectrum of Znfn1a1 (Ikaros) inactivation and its association with loss of heterozygosity in radiogenic T-cell lymphomas in susceptible B6C3F1 mice, Radiat. Res. 157 (2002) 331–340.

[16] P. Lopez-Nieva, J. Santos, J. Fernandez-Piqueras, Defective expression of Notch1 and Notch2 in connection to alterations of c-Myc and Ikaros in gamma-radiation-induced mouse thymic lymphomas, Carcinogenesis 25 (2004) 1299–1304.

[17] H. Okano, Y. Saito, T. Miyazawa, T. Shinbo, D. Chou, S. Kosugi, Y. Takahashi, S. Odani, O. Niwa, R. Kominami, Homozygous deletions and point mutations of the *Ikaros* gene in gamma-ray-induced mouse thymic lymphomas, Oncogene 18 (1999) 6677–6683.

[18] T. Shibuya, K. Morimoto, A review of the genotoxicity of 1-ethyl-1-nitrosourea, Mutat. Res. 297 (1993) 3–38.

[19] M.C. Poirier, R.M. Santella, A. Weston, Carcinogen macromolecular adducts and their measurement, Carcinogenesis 21 (2000) 353–359.

[20] E.W. Newcomb, J.J. Steinberg, A. Pellicer, *ras* oncogenes and phenotypic staging in *N*-methylnitrosourea- and gamma-irradiation-induced thymic lymphomas in C57BL/6J mice, Cancer Res. 48 (1988) 5514–5521.

[21] Y. Shimada, M. Nishimura, S. Kakinuma, T. Ogiu, H. Fujimoto, A. Kubo, J. Nagai, K. Kobayash, K. Tano, S. Yoshinaga, K.K. Bhakat, Genetic susceptibility to thymic lymphomas and K-*ras* gene mutation in mice after exposure to X-rays and *N*-ethyl-*N*-nitrosourea, Int. J. Radiat. Biol. 79 (2003) 423–430.

[22] E. Romach, J. Moore, S. Rummel, E. Richie, Influence of sex and carcinogen treatment protocol on tumor latency and frequency of K-*ras* mutations in *N*-methyl-*N*-nitrosourea-induced lymphomas, Carcinogenesis 15 (1994) 2275–2280.

[23] I.P. Perez de Castro, M. Malumbres, J. Santos, A. Pellicer, J. Fernandez-Piqueras, Cooperative alterations of Rb pathway regulators in mouse primary T cell lymphomas, Carcinogenesis 20 (1999) 1675–1682.

[24] S.W. Wijnhoven, P.P. Van Sloun, H.J. Kool, G. Weeda, R. Slater, P.H. Lohman, A.A. van Zeeland, H. Vrieling, Carcinogen-induced loss of heterozygosity at the Aprt locus in somatic cells of the mouse, Proc. Natl. Acad. Sci. U.S.A. 95 (1998) 13759–13764.

[25] S.W. Wijnhoven, H.J. Kool, C.M. van Teijlingen, A.A. van Zeeland, H. Vrieling, Loss of heterozygosity in somatic cells of the mouse. An important step in cancer initiation, Mutat. Res. 473 (2001) 23–36.

[26] M. Nishimura, S. Kakinuma, S. Wakana, A. Mukaigawara, K. Mita, T. Sado, T. Ogiu, Y. Shimada, Reduced sensitivity to and ras mutation spectrum of *N*-ethyl-*N*-nitrosourea-induced thymic lymphomas in adult C.B-17 scid mice, Mutat. Res. 486 (2001) 275–283.

[27] M. Nishimura, S. Wakana, S. Kakinuma, K. Mita, H. Ishii, S. Kobayashi, T. Ogiu, T. Sado, Y. Shimada, Low frequency of *Ras* gene mutation in spontaneous and gamma-ray-induced thymic lymphomas of scid mice, Radiat. Res. 151 (1999) 142–149.

[28] Y. Shimada, M. Nishimura, S. Kakinuma, T. Takeuchi, T. Ogiu, G. Suzuki, Y. Nakata, S. Sasanuma, K. Mita, T. Sado, Characteristic association between K-*ras* gene mutation with loss of heterozygosity in X-ray-induced thymic lymphomas of the B6C3F1 mouse, Int. J. Radiat. Biol. 77 (2001) 465–473.

[29] A. Karlsson, P. Soderkvist, S.M. Zhuang, Point mutations and deletions in the znfn1a1/*Ikaros* gene in chemically induced murine lymphomas, Cancer Res. 62 (2002) 2650–2653.

[30] K. Georgopoulos, Transcription factors required for lymphoid lineage commitment, Curr. Opin. Immunol. 9 (1997) 222–227.

[31] B.S. Cobb, S. Morales-Alcelay, G. Kleiger, K.E. Brown, A.G. Fisher, S.T. Smale, Targeting of Ikaros to pericentromeric heterochromatin by direct DNA binding, Genes Dev. 14 (2000) 2146–2160.

[32] A.M. Davidoff, P.A. Humphrey, J.D. Iglehart, J.R. Marks, Genetic basis for p53 overexpression in human breast cancer, Proc. Natl. Acad. Sci. U.S.A. 88 (1991) 5006–5010.

[33] O. Brathwaite, W. Bayona, E.W. Newcomb, p53 mutations in C57BL/6J murine thymic lymphomas induced by gamma-irradiation and *N*-methylnitrosourea, Cancer Res. 52 (1992) 3791–3795.

[34] A. Willis, E.J. Jung, T. Wakefield, X. Chen, Mutant p53 exerts a dominant negative effect by preventing wild-type p53 from binding to the promoter of its target genes, Oncogene 23 (2004) 2330–2338.

[35] G. Liu, T.J. McDonnell, R. Montes de Oca Luna, M. Kapoor, B. Mims, A.K. El-Naggar, G. Lozano, High metastatic potential in mice inheriting a targeted p53 missense mutation, Proc. Natl. Acad. Sci. U.S.A. 97 (2000) 4174–4179.

[36] A. de Vries, E.R. Flores, B. Miranda, H.M. Hsieh, C.T. van Oostrom, J. Sage, T. Jacks, Targeted point mutations of p53 lead to dominant-negative inhibition of wild-type p53 function, Proc. Natl. Acad. Sci. U.S.A. 99 (2002) 2948–2953.

[37] P. Papathanasiou, A.C. Perkins, B.S. Cobb, R. Ferrini, R. Sridharan, G.F. Hoyne, K.A. Nelms, S.T. Smale, C.C. Goodnow, Widespread failure of hematolymphoid differentiation caused by a recessive niche-filling allele of the Ikaros transcription factor, Immunity 19 (2003) 131–144.

[38] A.J. Paige, Redefining tumour suppressor genes: exceptions to the two-hit hypothesis, Cell Mol. Life Sci. 60 (2003) 2147–2163.

[39] P. Hohenstein, Tumour suppressor genes-one hit can be enough, PLoS Biol. 2 (2004) 40.

[40] H. Lee, D.S. Park, B. Razani, R.G. Russell, R.G. Pestell, M.P. *Lisanti*, Caveolin-1 mutations (P132L and null) and the pathogenesis of breast cancer: caveolin-1 (P132L) behaves in a dominant-negative manner and caveolin-1 (–/–) null mice show mammary epithelial cell hyperplasia, Am. J. Pathol. 161 (2002) 1357–1369.

[41] C. Kuang, Y. Chen, Tumor-derived C-terminal mutations of Smad4 with decreased DNA binding activity and enhanced intramolecular interaction, Oncogene 23 (2004) 1021–1029.

[42] M. Miyaki, T. Iijima, M. Konishi, K. Sakai, A. Ishii, M. Yasuno, T. Hishima, M. Koike, N. Shitara, T. Iwama, J. Utsunomiya, T. Kuroki, T. Mori, Higher frequency of *Smad4* gene mutation in human colorectal cancer with distant metastasis, Oncogene 18 (1999) 3098–3103.

[43] S. Venkatachalam, Y.P. Shi, S.N. Jones, H. Vogel, A. Bradley, D. Pinkel, L.A. Donehower, Retention of wild-type p53 in tumors from p53 heterozygous mice: reduction of p53 dosage can promote cancer formation, EMBO J. 17 (1998) 4657–4667.

[44] M.G. van Oijen, P.J. Slootweg, Gain-of-function mutations in the tumor suppressor gene *p53*, Clin. Cancer Res. 6 (2000) 2138–2145.

[45] A.I. Zaika, N. Slade, S.H. Erster, C. Sansome, T.W. Joseph, M. Pearl, E. Chalas, U.M. Moll, DeltaNp73, a dominant-negative inhibitor of wild-type p53 and TAp73, is up-regulated in human tumors, J. Exp. Med. 196 (2002) 765–780.

ANTIOXIDANTS & REDOX SIGNALING
Volume 6, Number 3, 2004

Forum Original Research Communication

Mitochondrial Signal Lacking Manganese Superoxide Dismutase Failed to Prevent Cell Death by Reoxygenation Following Hypoxia in a Human Pancreatic Cancer Cell Line, KP4

FUTOSHI HIRAI,[1,2] SHIGEATSU MOTOORI,[1] SHIZUKO KAKINUMA,[2] KAZUO TOMITA,[2,3] HIROKO P. INDO,[3] HIROTOSHI KATO,[2] TAKETO YAMAGUCHI,[1] HSIU-CHUAN YEN,[4] DARET K. ST. CLAIR,[5] TETSUO NAGANO,[6] TOSHIHIKO OZAWA,[2] HIROMITSU SAISHO,[1] and HIDEYUKI J. MAJIMA,[2,3,7]

ABSTRACT

One of the major characteristics of tumor is the presence of a hypoxic cell population, which is caused by abnormal distribution of blood vessels. Manganese superoxide dismutase (MnSOD) is a nuclear-encoded mitochondrial enzyme, which scavenges superoxide generated from the electron-transport chain in mitochondria. We examined whether MnSOD protects against hypoxia/reoxygenation (H/R)-induced oxidative stress using a human pancreas carcinoma-originated cell line, KP4. We also examined whether MnSOD is necessarily present in mitochondria to have a function. Normal human MnSOD and MnSOD without a mitochondrial targeting signal were transfected to KP4 cells, and reactive oxygen species, nitric oxide, lipid peroxidation, and apoptosis were examined as a function of time in air following 1 day of hypoxia as a H/R model. Our results showed H/R caused no increase in nitric oxide, but resulted in increases in reactive oxygen species, 4-hydroxy-2-nonenal protein adducts, and apoptosis. Authentic MnSOD protected against these processes and cell death, but MnSOD lacking a mitochondrial targeting signal could not. These results suggest that only when MnSOD is located in mitochondria is it efficient in protecting against cellular injuries by H/R, and they also indicate that mitochondria are primary sites of H/R-induced cellular oxidative injuries. *Antioxid. Redox Signal.* 6, 523–535.

INTRODUCTION

It has been known that hypoxic cells exist in tumors (7, 39) because of irregular localization of blood vessels. The hypoxic cells are resistant to various anticancer treatment modalities, such as radiation, bleomycin, *cis*-platinum, major chemotherapeutic agents utilized in the treatment of cancer, etc. (for review, see 16), which are all major treatments in cancer therapy. These treatment modalities are known to generate reactive oxygen species (ROS) (4, 30, 49). These modalities are effective in killing tumor cells; one of the mechanisms of tumor killing could be related to ROS

[1]First Department of Medicine, Chiba University, School of Medicine, Chiba 260–0856, Japan.
[2]National Institute of Radiological Sciences, Chiba 260-8555, Japan.
[3]Department of Oncology, Kagoshima University Graduate School of Medical and Dental Sciences, Kagoshima 890-8544, Japan.
[4]School of Medical Technology, Chang Gung University, Kwei-Shan, Tao-Yuan 333, Taiwan.
[5]Graduate Center for Toxicology, University of Kentucky, Lexington, KY 40536, U.S.A.
[6]Graduate School of Pharmaceutical Sciences, The University of Tokyo, Tokyo 113-0033, Japan.
[7]Department of Space Environmental Medicine, Kagoshima University Graduate School of Medical and Dental Sciences, Kagoshima 890-8544, Japan.

generation. Further, hypoxic cells may be related to the development of metastasis (31). Hypoxic cells often become reoxygenated after a dose of radiation or intermittent opening of blood vessels (6, 42). This phenomenon has been called reoxygenation (42).

Ischemia/reperfusion (I/R) in a normal brain causes oxidative damage to neuronal cells (for review, see 20, 25). Pathologic events caused by transient tissue hypoxia followed by oxygen reperfusion occur in numerous other tissues (for review, see 10). The pathologic changes encountered following reperfusion of an ischemic organ include an immediate generation of ROS, as well as subsequent inflammatory responses, which lead to a second stage of further ROS generation at the sites of damage. ROS generation following I/R has been examined in various experimental systems *in vivo* and *in vitro* (20). The injuries caused by I/R also occur in organ transplantation (10). One method to increase the effectiveness of organ transplantation may depend on methods to prevent oxidative stress. Clinical trials have been performed to determine whether antioxidant substances will prevent hypoxic-induced injury (10, 20). The use of gene therapy to reduce redox-mediated damage following such I/R injuries is also a subject for clinical consideration (10).

Many neuronal diseases, such as Alzheimer's disease, Parkinson's disease, and amyotrophic lateral sclerosis, and other diseases, such as aging, diabetes, premature babies, and cancer, are now believed to result from oxidative stress (12, 24, 43). Involvement of oxidative stress in tumor tissue is a subject of potentially great importance. Reoxygenation following hypoxia in tumor tissue has been implied to result in better prognosis after radiation therapy, although this hypoxia might also cause acceleration of tumor growth. However, how hypoxia/reoxygenation (H/R) affects tumor cell viability, and the subcellular mechanism(s) involved, have not been well elucidated. Possible changes in tumors may result from mitochondrial degeneration, as well as from subsequent ROS generation in cells (10). Several studies have shown that mitochondria produce superoxide, mainly from complex I and III of the electron transport system, which is located in the inner membrane of mitochondria (5, 36). Production of ROS from the electron transport chain may result in oxidative stress in cells, and may result in apoptotic cell death (23–25, 43). Manganese superoxide dismutase (MnSOD) is an essential enzyme, which scavenges superoxide located in mitochondria (44). The biological importance of MnSOD is demonstrated by the following: (a) A lack of the MnSOD gene in *Escherichia coli* and yeast makes them hypersensitive to oxidative stress (8, 11, 41). (b) Homozygous mutant mice lacking MnSOD died within the first 10 days after birth and showed dilated cardiomyopathy, an accumulation of lipid in the liver and skeletal muscle, and metabolic acidosis (21). (3) Mutant mice lacking MnSOD showed degenerative injury of large central nervous system neurons, particularly in the basal ganglia and brainstem, associated with damaged mitochondria. Also, these mice showed progressive motor disturbances characterized by limb weakness, rapid fatigue, and circling behavior (18). (d) Transfection of MnSOD cDNA into cultured cells rendered the cells resistant to paraquat- (32), tumor necrosis factor- (13, 47), doxorubicin- (13), mitomycin C- (13), radiation- (13, 27, 35), alkaline- (23), and chemical-induced hypoxia (15), cigarette smoke-induced cytotoxicity (34), and radiation-induced neoplastic transformation (33). (e) The expression of human MnSOD genes in transgenic mice protected the mice against oxygen-induced pulmonary injury (45) and adriamycin-induced cardiac toxicity (48). Thus, the expression of MnSOD is essential for the survival of aerobic life and the development of cellular resistance to oxygen radical-mediated toxicity.

MnSOD has a leader sequence to target mitochondria [mitochondrial targeting signal (MTS)]. This targeting signal translates to an oligopeptide consisting of 24 amino acids (14). The gene is transcribed in the nucleus, translated in the cytosol, and transported into mitochondria, where the precursor is cleaved and the protein undergoes maturation (22, 26). The localization of MnSOD in mitochondria is dependent on the presence of the signal. However, whether the enzyme could have an antioxidative function when it is present in the cytosol remains unclear.

In these studies, we examine the role of mitochondria-localized MnSOD in prevention against H/R-induced oxidative injuries, using a human pancreatic tumor-derived cell line, KP4, following H/R treatment. To elucidate further the significance of mitochondrial localization, MnSOD without the MTS gene was also tested using transfection in the same cell system.

MATERIALS AND METHODS

Cell lines

A pancreatic cancer cell line, KP4 (28), was purchased from the Riken Cell Bank (Tsukuba, Japan). pCR3.1-Uni plasmid (Invitrogen, Carlsbad, CA, U.S.A.) containing a sense human MnSOD cDNA insert was a *kind gift of* Dr. Akashi (National Institute of Radiological Sciences, Chiba, Japan) (27). A sequence analysis of the MnSOD gene in the construct showed that the sequence was identical to the accession number Y00472, except that C (nucleotide 113) was changed to T, and C (nucleotide 529) was changed to G, which changed alanine to valine and glutamine to glutamic acid, respectively (27). The KP4 cell was transfected using the GenePORTER transfection procedure (Gene Therapy Systems, San Diego, CA, U.S.A.) according to the manufacturer's instructions. In brief, cells were plated for 24 h before transfection at 60% confluence in a 60-mm dish. The cells were stably transfected with 5 μg of pCR3.1-Uni plasmids containing a sense human MnSOD cDNA insert, and linearized by Sca I, in a serum-free Dulbecco's modified Eagle medium (DMEM) (Life Technologies, Inc., Grand Island, NY, U.S.A.). The cells were also transfected with the same human MnSOD construct, but without an MTS [mito(−) MnSOD], which encodes 24 amino acids. The controls were transfected with pCR3.1-Uni plasmids without a human MnSOD cDNA insert and linearized by Sca I. Stable clones of both MnSOD and control plasmid transfectants were selected with Geneticin (Life Technologies, Inc.) at a final concentration of 500 μg/ml. Selected cellular clones that expressed MnSOD (MnSOD-5, -9, and -10), MnSOD without a targeting precursor [mito(−)-4, -6], selectable marker alone (vec-1 and -2),